Electronic Supplementary Material (ESI) for Nanoscale.


# SUPPLEMENTARY INFORMATION FOR

# Atomistic Understanding of Enhanced Selectivity in Photocatalytic Oxidation of Benzyl Alcohol to Benzaldehyde Using Graphitic Carbon Nitride Loaded with Single Copper Atoms

## A. Determination of photocatalytic performance

The photocatalytic performance, i.e., BA conversion, BAL yield, and BAL selectivity, was calculated using the following equations.

$$\text{Conversion}\ (\%) = \left(\frac{C_0 - C_r}{C_0}\right) \times 100 \quad (1)$$

$$\text{Yield}\ (\%) = \left(\frac{C_p}{C_0}\right) \times 100 \quad (2)$$

$$\text{Selectivity}\ (\%) = \left(\frac{C_p}{C_0 - C_r}\right) \times 100 \quad (3)$$

$$\text{Aromatic balance}\ (\%) = \left(\frac{C_r + C_p}{C_0}\right) \times 100 \quad (4)$$

where $C_0$ is the initial BA concentration (mmol $L^{-1}$). $C_r$ and $C_p$ are the concentration of reactant (BA) and product (BAL) when sampling, respectively.

## B. Experimental results

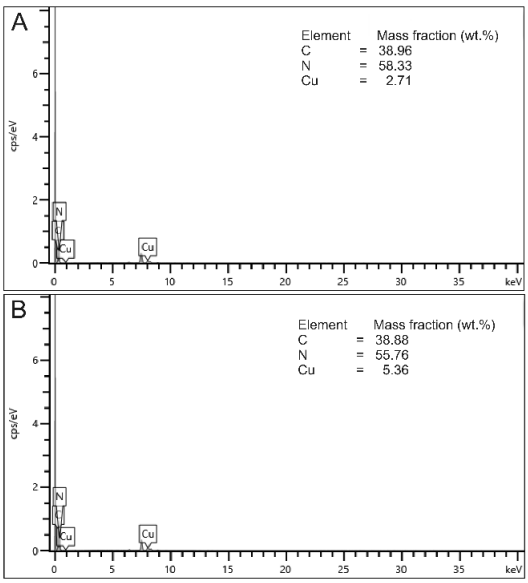


**Figure S1.** EDS spectra of (A) 3Cu-CN and (B) 6Cu-CN.

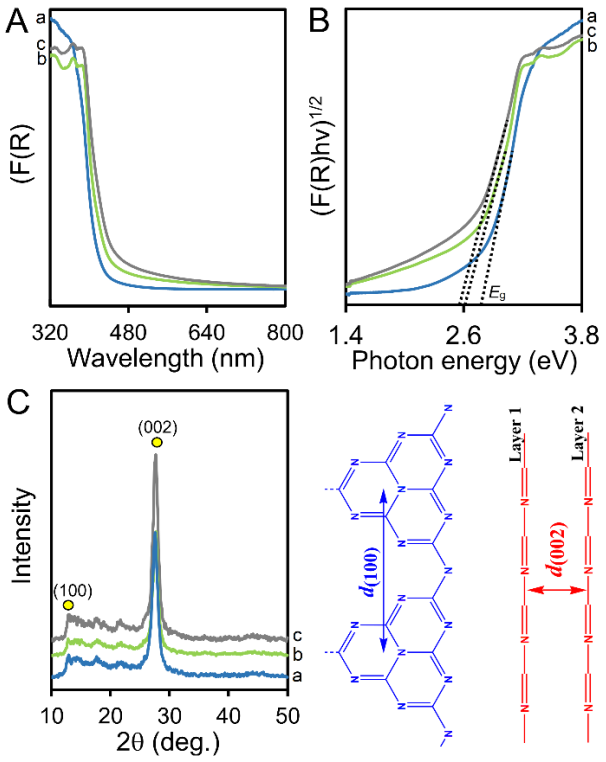


**Figure S2.** (A) DR spectra, (B) Tauc's plots, and (C) XRD patterns with the structural assignment of the diffraction peaks of (a) CN, (b) 3Cu-CN, and (c) 6Cu-CN.

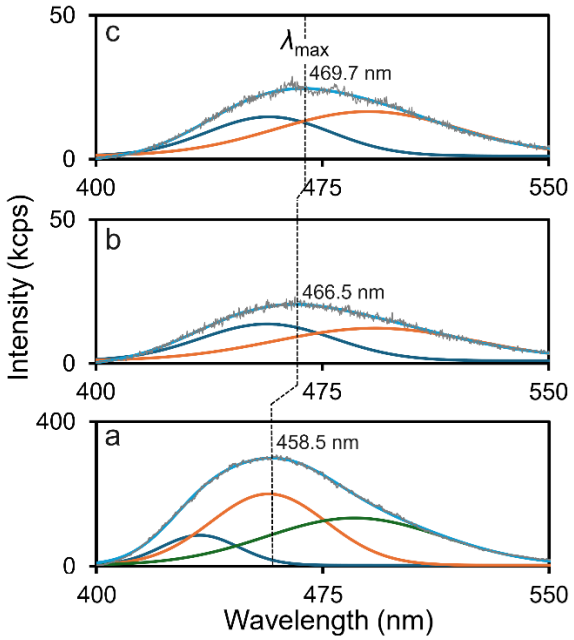


**Figure S3.** PL spectra of (a) CN, (b) 3Cu-CN, and (c) 6Cu-CN.

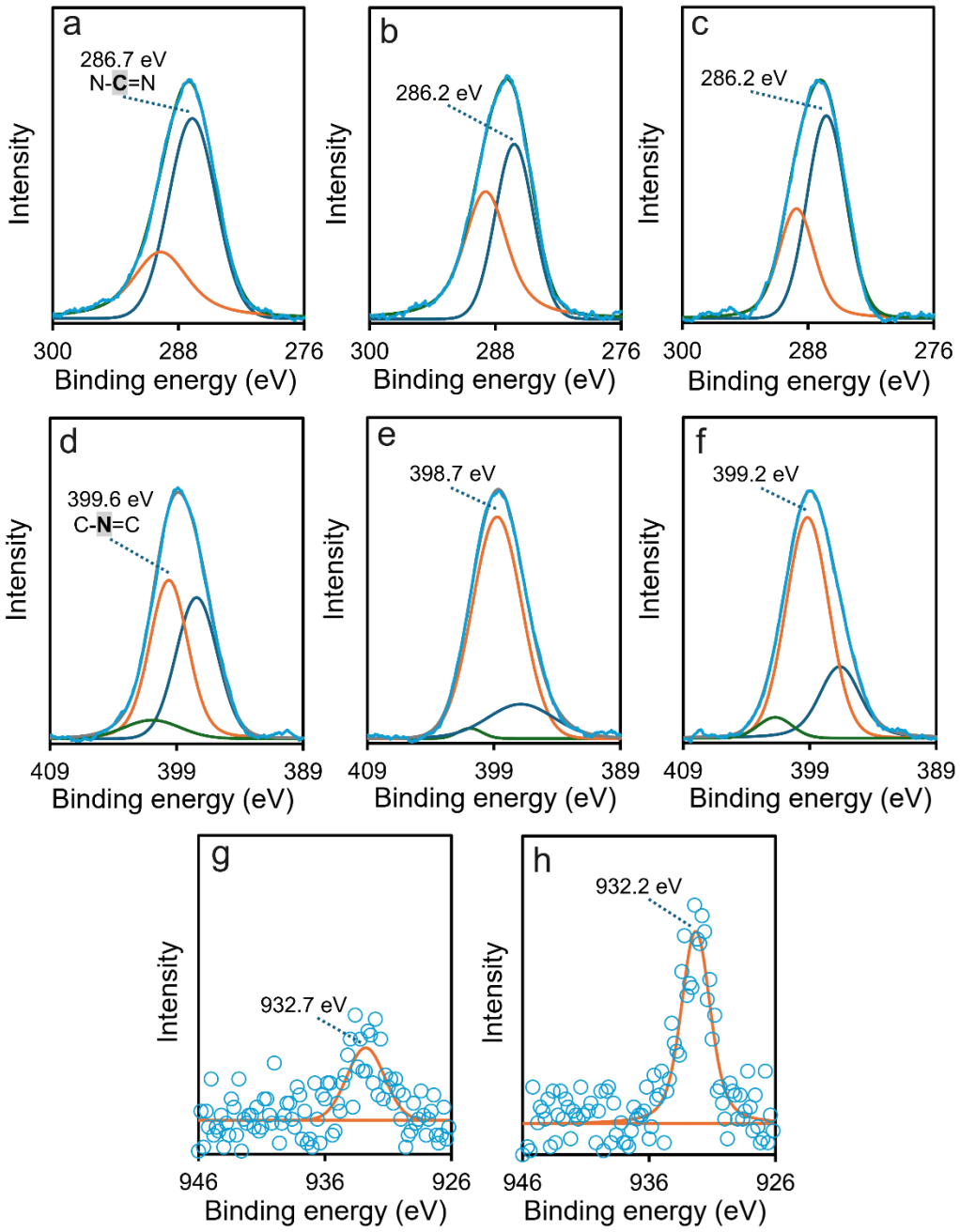


**Figure S4.** XPS spectra of CN at (a) C 1s and (d) N 1s regions, 3Cu-CN at (b) C 1s, (e) N 1s, and (g) Cu 2p3/2, and 6Cu-CN at (c) C 1s, (f) N 1s, and (h) Cu 2p3/2 regions.

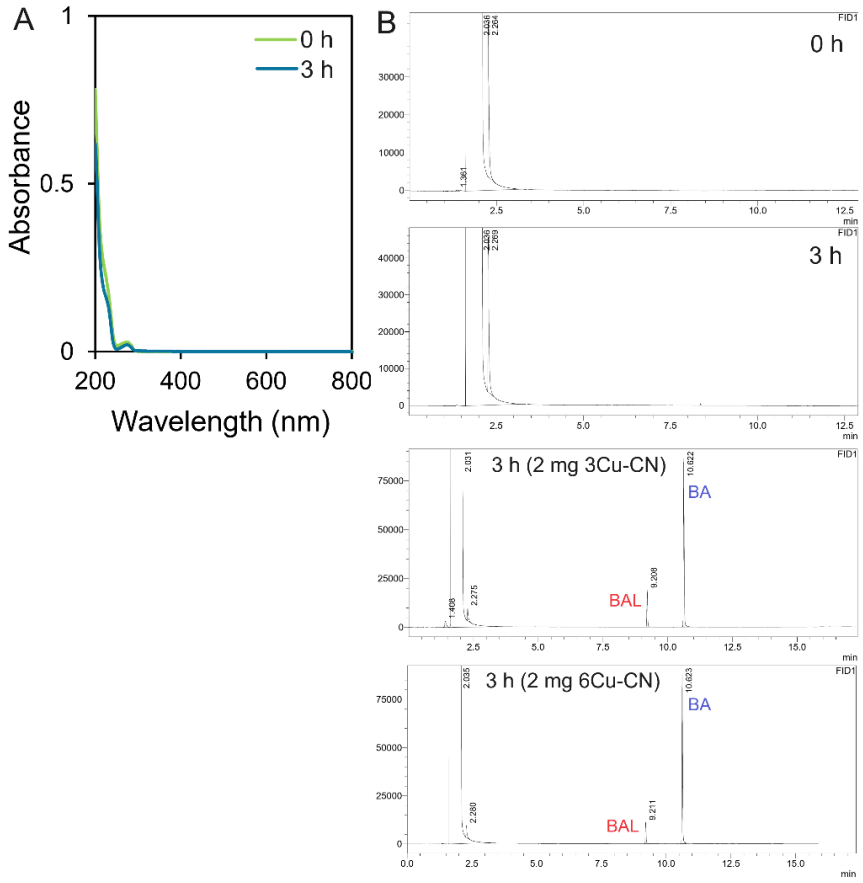


**Figure S5.** (A) UV-Vis absorption and (B) gas chromatogram of fresh acetonitrile and after being exposed to visible light for 3 h without photocatalyst. Chromatograms of the reaction medium after 3 h of light irradiation with Cu-CN samples, where BAL is the only reaction product present, are also shown.

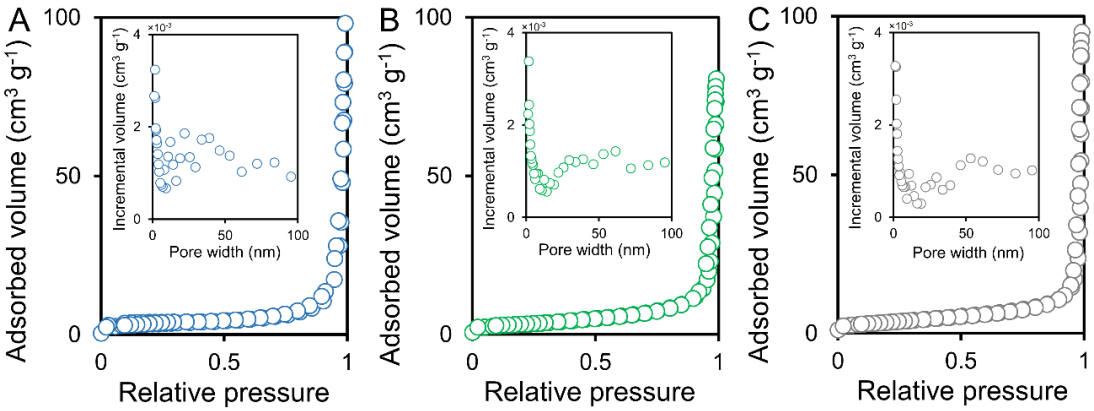


**Figure S6.** $N_2$ adsorption−desorption isotherms of (A) CN, (B) 3Cu-CN, and (C) 6Cu-CN. The insets are the corresponding pore-size distribution curves.

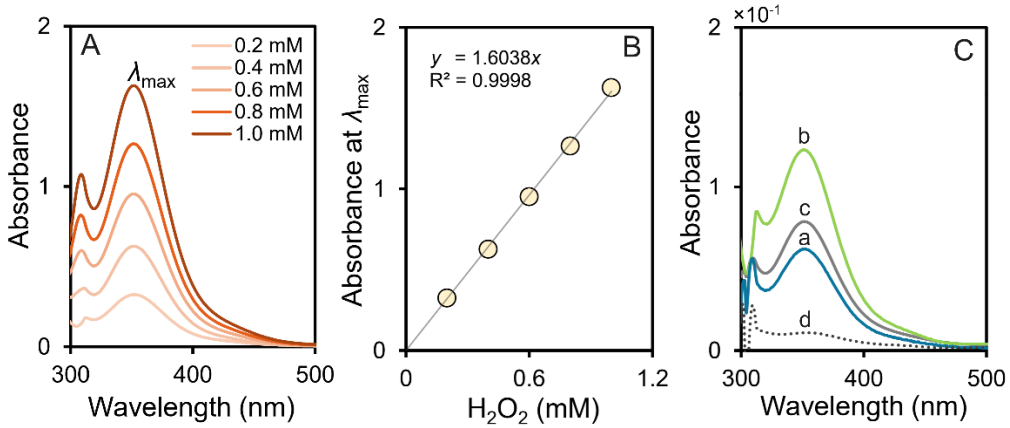


**Figure S7.** (A) UV-Vis absorption intensity of different standard concentrations of $H_2O_2$ determined using the iodometric method. (B) Linear fitting for standard $H_2O_2$ concentrations. (C) UV-Vis absorption spectra for (a) CN, (b) 3Cu-CN, (c) 6Cu-CN, and (d) BA in acetonitrile under light exposure without photocatalyst.

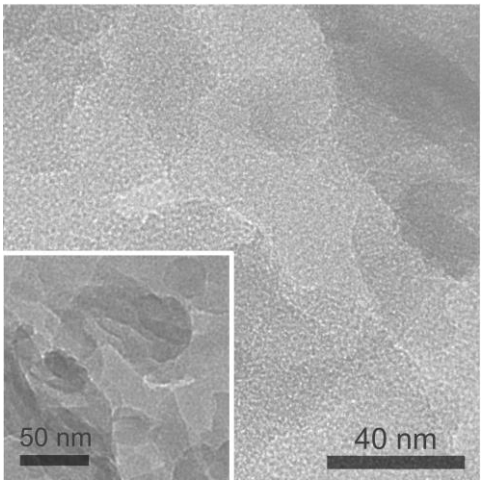


**Figure S8.** TEM images of 6Cu-CN.

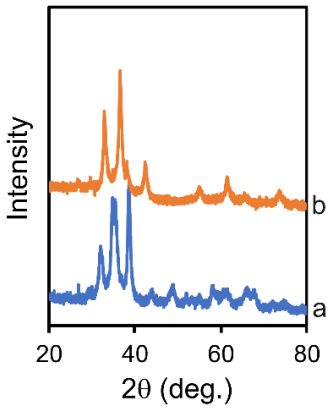


**Figure S9.** XRD patterns of (a) $Cu_2O$ and (b) CuO.

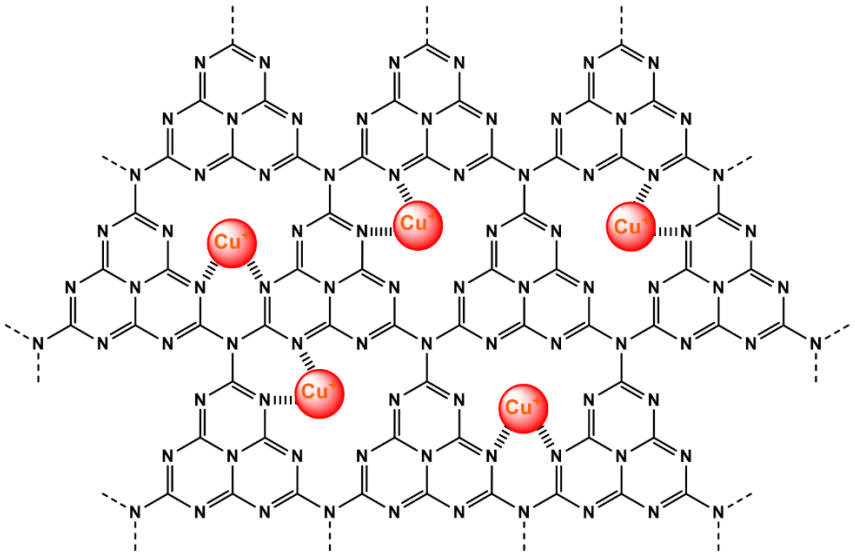


**Figure S10.** Proposed structure of a heptazine-based layer with low-coordinated $Cu^+$ cations in 3Cu-CN. Based on the AIMD simulation, the gCN layer is not planar at 27 ºC but irregularly curved, making its cavities (and thus the length of the Cu-N coordination) unsymmetrical and the Cu-N coordination to exist in more than one configuration.

**Table S1.** Partial oxidation of benzyl alcohol over $gC_3N_4$-based photocatalysts

| Catalyst | Precursor[a] | $S_{BET}$ ($m^2\ g^{-1}$) | Con. ($g\ L^{-1}$) | Light source | *t* (h) | *T* (°C) | BA con. (mmol $L^{-1}$) | BA conv. (%) | BAL sel. (%)[b] | Yield-to-Power ratio (mmol BAL $g^{-1}\ h^{-1}\ W^{-1}$) | Ref. |
|---|---|---|---|---|---|---|---|---|---|---|---|
| P-$gC_3N_4$ | Melamine | 4 | 0.33 | Fluorescent lamps (3 ×15 W, 340-420 nm) | 4 | 25 | 500 (acetonitrile) | 5 | 52 | 0.21 | [1] |
| P-$gC_3N_4$ | Urea | 16 | | | | | | 4 | 45 | 0.15 | |
| P-$gC_3N_4$ | Thiourea | 28 | | | | | | 3 | 36 | 0.09 | |
| Pt@$gC_3N_4$ | Melamine | 6 | 0.625 | Xe lamp (200 W, ≥420 nm, | 5 | *n.a.* | 10 (water) | 27 | 90 | <0.01 | [2] |
| P/$gC_3N_4$ | Urea | *n.a.* | 2 | LED lamp (64 W, 465 nm) | 10 | 25 | 50 (acetonitrile, $O_2$) | 96 | >99 | 0.04 | [3] |
| $gC_3N_4$ | Melamine | *n.a.* | 0.67 | Fluorescent lamps (6 × 15 W, 315-400 nm) | 4 | 25 | 0.5 (water) | 29 | 88 | <0.01 | [4] |
| $gC_3N_4$ | Cyanamide | 130 | 2.5 | Xe lamp (300 W, >420 nm) | 3 | 100 | 40 (water, 0.8 MPa $O_2$) | 10 | 96 | <0.01 | [5] |
| CdS/$gC_3N_4$ | Melamine | 7 | 6.67 | Xe lamp (300 W, >420 nm) | 4 | 60 | 25.5 (benzotrifluoride, 0.5 MPa $N_2$) | 48 | 93 | <0.01 | [6] |
| S-$gC_3N_4$ | Dicyandiamide | 66 | 5 | Xe lamp (300 W, >420 nm) | 4 | 100 | 100 (trifluorotoluene, 0.1 MPa $O_2$) | 19 | >99 | <0.01 | [7] |
| $gC_3N_4$ | Cyanamide | 200 | 5 | Xe lamp (300 W, >420 nm) | 3 | 100 | 100 (acetonitrile, 0.8 MPa $O_2$) | 70 | 68 | 0.01 | [8] |
| NHPI/$gC_3N_4$* | Cyanamide | *n.a.* | 10 | W-filament bulb (250 W, >420 nm) | 22 | 25 | 500 (toluene, 5 mL $min^{-1}$ $O_2$) | 89 | 94 | <0.01 | [9] |
| $gC_3N_4$ | Melamine | *n.a.* | 3.75 | Hg lamp (100 W, >400 nm) | 3 | 25 | 25 (water, $O_2$) | 96 | 82 | 0.02 | [10] |
| $gC_3N_4$ | Melamine | 43 | 1.67 | LED lamps (18 × 1 W, 395 nm) | 5 | 20 | 2 (acetonitrile) | 77 | 87 | <0.01 | [11] |
| $gC_3N_4$ | Urea | 53 | | | | | | 85 | 85 | <0.01 | |
| Fe@$gC_3N_4$ | Melamine | *n.a.* | 2.5 | LED lamp (18 W, >400 nm) | 3 | 25 | 200 (acetonitrile, 3 mL $H_2O_2$) | 93 | >99 | 1.36 | [12] |
| MIL/Ag/$gC_3N_4$ | Melamine | 101 | 0.83 | Xe lamp (500 W, >400 nm) | 6 | 25 | 33.4 (water, $O_2$) | 47 | 97 | <0.01 | [13] |
| $TiO_2$/$gC_3N_4$ | Urea | 68 | 2.5 | Xe lamp (400 W, >400 nm) | 4 | 50 | 100 (acetonitrile, $O_2$) | 42 | >99 | 0.01 | [14] |
| Ru@B-$gC_3N_4$ | Melamine | 2.5 | 0.5 | UVA lamp (2×18 W, 365 nm) | 3 | 20 | 0.5 (water) | 83 | 57 | <0.01 | [15] |
| $Fe_2O_3$/$gC_3N_4$ | Melamine | 27 | 1 | Hg lamp (125 W, 365 nm) | 4 | 30 | 100 (acetonitrile, 25 mL $min^{-1}$ $O_2$) | 20 | 34 | 0.01 | [16] |
| ZnO/$gC_3N_4$ | Melamine | 10 | | | | | | 9 | 26 | <0.01 | |
| Cu@$gC_3N_4$ | Dicyandiamide | 13 | 0.5 | LED lamp (0.45 W, 465 nm) | 3 | 25 | 1 (acetonitrile) | 25 | 96 | 0.35 | This work |

*N-hydroxyphthalimide (NHPI). [a]Precursor for the $gC_3N_4$. [b]Selectivity to BAL. [c]Not available.

**Table S2.** Recycling tests for the BA oxidation

| Photocatalyst | Cycle | BA conv. (%) | BAL yield (%) | BAL sel. (%) |
|---|---|---|---|---|
| CN | 1 | 15 | 3 | 20 |
| | 2 | 16 | 3 | 19 |
| | 3 | 15 | 2 | 13 |
| | 4 | 13 | 2 | 15 |
| *Stored for 8 months* | | 18 | 3 | 17 |
| 3Cu-CN | 1 | 25 | 24 | 96 |
| | 2 | 24 | 22 | 92 |
| | 3 | 25 | 24 | 96 |
| | 4 | 28 | 25 | 90 |
| *Stored for 8 months* | | 28 | 26 | 93 |
| 6Cu-CN | 1 | 21 | 17 | 81 |
| | 2 | 20 | 16 | 80 |
| | 3 | 20 | 17 | 85 |
| | 4 | 18 | 14 | 78 |
| *Stored for 8 months* | | 20 | 16 | 80 |

Reaction conditions: BA (1 mmol $L^{-1}$, 0.01 mmol), photocatalyst (0.5 g $L^{-1}$, 5 mg), and reaction time (3 h).

**Table S3.** Partial oxidation of BA over CN in the presence of scavengers

| Scavenger | BA conv. (%) | BAL yield (%) | BAL sel. (%) |
|---|---|---|---|
| none | 15 | 3 | 20 |
| $AgNO_3$ | 13 | 2 | 15 |
| $Na_2SO_4$ | 12 | 2 | 17 |
| KI | 14 | 2 | 14 |
| BQ | 10 | 1 | 10 |
| *t*-butanol | 15 | 3 | 20 |

Reaction conditions: BA (1 mmol $L^{-1}$, 0.01 mmol), scavenger (5 mmol $L^{-1}$, 0.05 mmol), photocatalyst (0.5 g $L^{-1}$, 5 mg), and reaction time (3 h).

**Table S4.** Partial oxidation of BA over 3Cu-CN in the presence of scavengers

| Scavenger | BA conv. (%) | BAL yield (%) | BAL sel. (%) |
|---|---|---|---|
| none | 25 | 24 | 96 |
| $AgNO_3$ | 18 | 15 | 83 |
| $Na_2SO_4$ | 22 | 18 | 82 |
| KI | 13 | 10 | 77 |
| BQ | 20 | 16 | 80 |
| *t*-butanol | 24 | 22 | 92 |

Reaction conditions: BA (1 mmol $L^{-1}$, 0.01 mmol), scavenger (5 mmol $L^{-1}$, 0.05 mmol), photocatalyst (0.5 g $L^{-1}$, 5 mg), and reaction time (3 h).

**Table S5.** Partial oxidation of BA over 6Cu-CN in the presence of scavengers

| Scavenger | BA conv. (%) | BAL yield (%) | BAL sel. (%) |
|---|---|---|---|
| none | 21 | 17 | 81 |
| $AgNO_3$ | 16 | 11 | 69 |
| $Na_2SO_4$ | 19 | 14 | 73 |
| KI | 18 | 12 | 67 |
| BQ | 18 | 13 | 72 |
| *t*-butanol | 20 | 16 | 80 |

Reaction conditions: BA (1 mmol $L^{-1}$, 0.01 mmol), scavenger (5 mmol $L^{-1}$, 0.05 mmol), photocatalyst (0.5 g $L^{-1}$, 5 mg), and reaction time (3 h).

**Table S6.** Partial oxidation of BA in the presence of hole scavengers

| Scavenger | Photocatalyst | BA conv. (%) | BAL yield (%) | BAL sel. (%) |
|---|---|---|---|---|
| none | CN | 15 | 3 | 20 |
| | 3Cu-CN | 25 | 24 | 96 |
| | 6Cu-CN | 21 | 17 | 81 |
| KI | CN | 14 | 2 | 14 |
| | 3Cu-CN | 13 | 10 | 77 |
| | 6Cu-CN | 18 | 12 | 67 |
| TEMPO | CN | 12 | 2 | 17 |
| | 3Cu-CN | 7 | 6 | 85 |
| | 6Cu-CN | 7 | 5 | 71 |
| OA | CN | 13 | 2 | 15 |
| | 3Cu-CN | 14 | 13 | 93 |
| | 6Cu-CN | 15 | 12 | 80 |

Reaction conditions: BA (1 mmol $L^{-1}$, 0.01 mmol), scavenger (5 mmol $L^{-1}$, 0.05 mmol), photocatalyst (0.5 g $L^{-1}$, 5 mg), and reaction time (3 h).

**Table S7.** Partial oxidation of BA over 3Cu-CN with different reaction conditions

| Scavenger(s) | Concentration (mmol $L^{-1}$) | BA conv. (%) | BAL yield (%) | BAL sel. (%) |
|---|---|---|---|---|
| BQ | 0 | 25 | 24 | 96 |
| | 0 ($O_2$ flow, 25 mL $min^{-1}$, 1 h) | 30 | 26 | 87 |
| | 0 (Ultrasonic degassing, 0.5 h, followed by Ar flow, 25 mL $min^{-1}$, 1 h) | 19 | 16 | 84 |
| | 2 | 21 | 17 | 81 |
| | 4 | 19 | 17 | 89 |
| | 8 | 16 | 14 | 87 |
| BQ + KI | 4 + 4 | 3 | 0 | 0 |
| BQ + TEMPO | 4 + 4 | 0 | 0 | 0 |
| BQ + OA | 4 + 4 | 6 | 4 | 67 |

Reaction conditions: BA (1 mmol $L^{-1}$, 0.01 mmol), photocatalyst (0.5 g $L^{-1}$, 5 mg), and reaction time (3 h).

**Table S8.** $H_2O_2$ production determined based on the iodometric method [17-19]

$$H_2O_2 + 3I^- + 2H^+ \rightarrow I_3^- + 2H_2O$$

| | Photocatalyst | $H_2O_2$ (μM $h^{-1}$) | Yield-to-Power ratio (mmol $g^{-1}$ $h^{-1}$ $W^{-1}$) | Ref. |
|---|---|---|---|---|
| No light | CN | 0 | 0 | |
| No catalyst | - | 2 | 1 | |
| | CN | 13 | 9 | |
| | 3Cu-CN | 25 | 17 | |
| | 6Cu-CN | 16 | 11 | |
| | Ni-CN | 342 | 236 | [17] |

Reaction conditions: BA (1 mmol $L^{-1}$, 0.01 mmol), photocatalyst (0.5 g $L^{-1}$, 5 mg), visible light 300 mW at 465 nm, and reaction time (3 h).

## References


1. Bellardita M, García-López EI, Marcì G, Krivtsov I, García JR, Palmisano L: **Selective photocatalytic oxidation of aromatic alcohols in water by using P-doped g-$C_3N_4$**. *Applied Catalysis B: Environmental* 2018, **220**:222-233.
2. Huo T, Deng Q, Yu F, Wang G, Xia Y, Li H, Hou W: **Ion-Induced Synthesis of Crystalline Carbon Nitride Ultrathin Nanosheets from Mesoporous Melon for Efficient Photocatalytic Hydrogen Evolution with Synchronous Highly Selective Oxidation of Benzyl Alcohol**. *ACS Applied Materials & Interfaces* 2022, **14**(11):13419-13430.

3. Pahari SK, Doong R-A: **Few-layered phosphorene–graphitic carbon nitride nanoheterostructure as a metal-free photocatalyst for aerobic oxidation of benzyl alcohol and toluene**. *ACS Sustainable Chemistry & Engineering* 2020, **8**(35):13342-13351.
4. Krivtsov I, Ilkaeva M, García-López EI, Marcì G, Palmisano L, Bartashevich E, Grigoreva E, Matveeva K, Díaz E, Ordóñez S: **Effect of substituents on partial photocatalytic oxidation of aromatic alcohols assisted by polymeric $C_3N_4$**. *ChemCatChem* 2019, **11**(11):2713-2724.
5. Long B, Ding Z, Wang X: **Carbon nitride for the selective oxidation of aromatic alcohols in water under visible light**. *ChemSusChem* 2013, **6**(11):2074-2078.
6. Dai X, Xie M, Meng S, Fu X, Chen S: **Coupled systems for selective oxidation of aromatic alcohols to aldehydes and reduction of nitrobenzene into aniline using CdS/g-$C_3N_4$ photocatalyst under visible light irradiation**. *Applied Catalysis B: Environmental* 2014, **158**:382-390.
7. Zhang L, Liu D, Guan J, Chen X, Guo X, Zhao F, Hou T, Mu X: **Metal-free g-$C_3N_4$ photocatalyst by sulfuric acid activation for selective aerobic oxidation of benzyl alcohol under visible light**. *Materials Research Bulletin* 2014, **59**:84-92.
8. Su F, Mathew SC, Lipner G, Fu X, Antonietti M, Blechert S, Wang X: **mpg-$C_3N_4$-catalyzed selective oxidation of alcohols using $O_2$ and visible light**. *Journal of the American Chemical Society* 2010, **132**(46):16299-16301.
9. Zhang P, Deng J, Mao J, Li H, Wang Y: **Selective aerobic oxidation of alcohols by a mesoporous graphitic carbon nitride/N-hydroxyphthalimide system under visible-light illumination at room temperature**. *Chinese Journal of Catalysis* 2015, **36**(9):1580-1586.
10. Shvalagin V, Kompanets M, Kutsenko O, Kuchmy SY, Skoryk M: **Photocatalytic Activity of g$C_3N_4$ in the Partial Oxidation of Benzyl Alcohol Under Visible Light**. *Theoretical and Experimental Chemistry* 2020, **56**:111-116.
11. Morozov R, Golovin M, Uchaev D, Fakhrutdinov A, Gavrilyak M, Arkhipushkin I, Boronin V, Korshunov V, Podgornov F, Taydakov I: **Polytriazine imide-LiCl semiconductor for highly efficient photooxidation of benzyl alcohol to benzaldehyde**. *Journal of Chemical Sciences* 2021, **133**:1-17.
12. Devi M, Ganguly S, Bhuyan B, Dhar SS, Vadivel S: **A novel [Fe (acac)3] interspersed g-$C_3N_4$ heterostructure for environmentally benign visible-light-driven oxidation of alcohols**. *European Journal of Inorganic Chemistry* 2018, **2018**(44):4819-4825.
13. Yang Z, Xu X, Liang X, Lei C, Cui Y, Wu W, Yang Y, Zhang Z, Lei Z: **Construction of heterostructured MIL-125/Ag/g-$C_3N_4$ nanocomposite as an efficient bifunctional visible light photocatalyst for the organic oxidation and reduction reactions**. *Applied catalysis B: environmental* 2017, **205**:42-54.
14. Mohammadi M, Hadadzadeh H, Kaikhosravi M, Farrokhpour H, Shakeri J: **Selective photocatalytic oxidation of benzyl alcohol at ambient conditions using spray-dried g-$C_3N_4$/$TiO_2$ granules**. *Molecular Catalysis* 2020, **490**:110927.
15. Solís RR, Quintana MA, Blázquez G, Calero M, Muñoz-Batista MJ: **Ruthenium deposited onto graphitic carbon modified with boron for the intensified photocatalytic production of benzaldehyde**. *Catalysis Today* 2023, **423**:114266.
16. Cerdan K, Ouyang W, Colmenares JC, Munoz-Batista MJ, Luque R, Balu AM: **Facile mechanochemical modification of g-$C_3N_4$ for selective photo-oxidation of benzyl alcohol**. *Chemical Engineering Science* 2019, **194**:78-84.
17. Zhang X, Su H, Cui P, Cao Y, Teng Z, Zhang Q, Wang Y, Feng Y, Feng R, Hou J: **Developing Ni single-atom sites in carbon nitride for efficient photocatalytic $H_2O_2$ production**. *Nature Communications* 2023, **14**(1):7115.
18. Zhang X, Ma P, Wang C, Gan L, Chen X, Zhang P, Wang Y, Li H, Wang L, Zhou X: **Unraveling the dual defect sites in graphite carbon nitride for ultra-high photocatalytic $H_2O_2$ evolution**. *Energy & Environmental Science* 2022, **15**(2):830-842.
19. Wei Z, Liu M, Zhang Z, Yao W, Tan H, Zhu Y: **Efficient visible-light-driven selective oxygen reduction to hydrogen peroxide by oxygen-enriched graphitic carbon nitride polymers**. *Energy & Environmental Science* 2018, **11**(9):2581-2589.

20. Bhoyar T, Abraham BM, Gupta A, Kim DJ, Manwar NR, Pasupuleti KS, Vidyasagar D, Umare SS: **Counterion chemistry of 5-halo (X: Cl, Br, I)-uracil derived carbon nitride: unlocking enhanced photocatalytic performance**. *Journal of Materials Chemistry A* 2024, **12**(2):979-992.